Available online at www.sciencedirect.com
SCIENCE DIRECT®
Journal of Sound and Vibration 272 (2004) 1125–1133
JOURNAL OF SOUND AND VIBRATION
www.elsevier.com/locate/jsvi

Letter to the Editor

Sound attenuation in dissipative expansion chambers

M.B. Xu[a,b], A. Selamet[a,b,*], I.-J. Lee[a,b], N.T. Huff[c]

[a] *Department of Mechanical Engineering, The Ohio State University, Columbus, OH 43210-1107, USA*
[b] *The Center for Automotive Research, The Ohio State University, Columbus, OH 43212-1443, USA*
[c] *Owens Corning Automotive, Novi, MI 48377, USA*

Received 21 July 2003; accepted 23 July 2003

1. Introduction

Recent improvements in fiber properties combined with their broadband acoustic dissipation characteristics make such materials potentially desirable for implementation in silencers. The acoustic modelling of simple silencer geometries, such as circular or rectangular cross-sections, has been established and classified depending on the assumption of locally- or bulk-reacting lining. Morse [1] used a locally-reacting model to investigate the sound transmission in pipes with absorbing material on the inner walls. By using bulk-reacting model for linings, Scott [2] studied the transmission of sound in infinite rectangular and circular ducts; Ko [3] investigated the characteristics of sound attenuation for rectangular, annular and circular ducts; Cummings and Chang [4] examined the effect of mean flow on the modal attenuation rates.

The foregoing investigations [1–4] have targeted infinitely long ducts, thereby excluding the effects associated with the expansion/contraction of a finite chamber. In order to fully understand the acoustic performance of a finite-length dissipative silencer, it is essential to investigate the effect of discontinuities across the expansion/contraction of the expansion chamber. Cummings and Chang [5] analyzed the sound attenuation of a finite length dissipative silencer with mean flow by using a mode-matching technique. Axial acoustic particle velocity and pressure were matched across the expansion/contraction of the chamber, and a good agreement between predictions and measurements was observed. Peat [6] developed a transfer matrix formulation for the bulk-reacting dissipative silencer from the match of average acoustic pressure/velocity across the silencer discontinuities. By using one-dimensional analytical approach, three-dimensional BEM, and experimental methods, the acoustic attenuation was discussed for both a single-pass dissipative expansion chamber [7] and a hybrid silencer [8] consisting of two single-pass dissipative expansion chambers and a Helmholtz resonator. A pod silencer, which is a lined circular duct with

*Corresponding author. Department of Mechanical Engineering, The Ohio State University, 206 West 18th Avenue, Columbus, OH 43210-1107, USA. Tel.: +1-614-292-4143; fax: +1-614-292-3163.
E-mail address: selamet.1@osu.edu (A. Selamet).

0022-460X/$ - see front matter
doi:10.1016/j.jsv.2003.07.025

a cylindrical pod inside, was also investigated; and both the four-pole parameters and transmission loss were obtained by plane-wave analysis [9].

In Refs. [5–8], the diameter of the airway in the dissipative expansion chamber is always set equal to that of the inlet/outlet pipes. In Ref. [9], this diameter is different than that of the inlet/outlet pipes, however, only a plane-wave analysis is provided. Using a two-dimensional analytical approach, the present study examines the effect of fiber thickness, chamber diameter, and material properties on the acoustic performance of dissipative silencers. An analytical approach is proposed based on the solution of eigenequation for a circular dissipative expansion chamber. The acoustic pressure and particle velocity across the silencer discontinuities are matched by imposing the continuities of the velocity/pressure integral over discrete zones at the expansion/contraction. The analytical results are shown to agree well with the numerical predictions and measurements.

2. Theory

Consider a cylindrical dissipative silencer of length L and radius r_3, with sound-absorbing material placed between radii r_2 and r_3, as shown in Fig. 1. The inlet and outlet of radius r_1 are designated by domains I and III, and the chamber by domain II. The absorbing material is assumed to be homogeneous and isotropic, characterized by the complex speed of sound $\tilde{c}$ and density $\tilde{\rho}$.

In the inlet pipe (domain I), the solution to the Helmholtz equation

$$\frac{\partial^2 P}{\partial r^2}+\frac{1}{r}\frac{\partial P}{\partial r}+\frac{\partial^2 P}{\partial x^2}+k_0^2 P=0 \tag{1}$$

can be written as

$$P_A(r,x)=\sum_{n=0}^{\infty}(A_n^+ \mathrm{e}^{-\mathrm{j}k_{x,A,n}x}+A_n^- \mathrm{e}^{\mathrm{j}k_{x,A,n}x})\psi_{A,n}(r) \tag{2}$$

with P_A being the acoustic pressure in domain I; $k_0=2\pi f/c_0$ is the wavenumber in air with c_0 being the speed of sound and f the frequency; A_n^+ and A_n^- the modal amplitudes corresponding to components travelling in the positive and negative x directions, respectively; $k_{x,A,n}$ the wavenumber in x direction, and the subscript x, A, n denotes axial direction, domain I, and order of the waves, respectively;

$$\psi_{A,n}(r)=\mathrm{J}_0(k_{r,A,n}r) \tag{3}$$

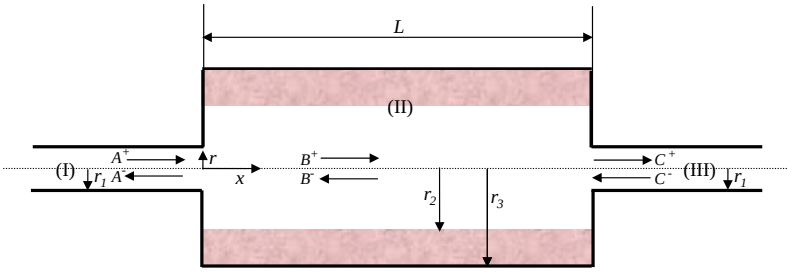

Fig. 1. Geometry of a cylindrical dissipative expansion chamber.

is the eigenfunction for this circular duct, with J_0 being the zeroth order Bessel function of the first kind, $k_{r,A,n}$ the radial wavenumber satisfying the rigid wall boundary condition of

$$J_0'(k_{r,A,n}r_1) = 0. \tag{4}$$

The axial wavenumber of the n-mode is

$$k_{x,A,n} = \begin{cases} \sqrt{k_0^2 - k_{r,A,n}^2}, & k_0 > k_{r,A,n}, \\ -\sqrt{k_0^2 - k_{r,A,n}^2}, & k_0 < k_{r,A,n} \end{cases} \tag{5}$$

with the negative sign being assigned so that $e^{-jk_{x,A,n}x}$ decays exponentially in x direction.

The particle velocity in x direction may then be written, in terms of the linearized momentum equation, as

$$u_{x,A}(r,x) = \frac{1}{\rho_0\omega}\sum_{n=0}^{\infty} k_{x,A,n}(A_n^+ e^{-jk_{x,A,n}x} - A_n^- e^{jk_{x,A,n}x})\psi_{A,n}(r), \tag{6}$$

where ρ_0 is the density of air and ω the angular velocity.

In the outlet pipe (domain III), the acoustic pressure and axial velocity are similar to those in the inlet pipe (domain I), and can be expressed as

$$P_C(r,x) = \sum_{n=0}^{\infty} (C_n^+ e^{-jk_{x,C,n}(x-L)} + C_n^- e^{jk_{x,C,n}(x-L)})\psi_{C,n}(r) \tag{7}$$

and

$$u_{x,C}(r,x) = \frac{1}{\rho_0\omega}\sum_{n=0}^{\infty} k_{x,C,n}(C_n^+ e^{-jk_{x,C,n}(x-L)} - C_n^- e^{jk_{x,C,n}(x-L)})\psi_{C,n}(r), \tag{8}$$

where subscript C denotes domain III, C_n^+ and C_n^- are the amplitudes; and the eigenfunction, $\psi_{C,n}(r)$ and wavenumber, $k_{x,C,n}$ are similar to those in the inlet pipe.

The sound propagation in the dissipative expansion chamber (domain II) is also governed by

$$\frac{\partial^2 P}{\partial r^2} + \frac{1}{r}\frac{\partial P}{\partial r} + \frac{\partial^2 P}{\partial x^2} + \kappa^2 P = 0, \tag{9}$$

where

$$\kappa = \begin{cases} k_0, & 0 \leqslant r \leqslant r_2, \\ \tilde{k}, & r_2 \leqslant r \leqslant r_3 \end{cases} \tag{10}$$

with $\tilde{k} = 2\pi f/\tilde{c}$ denoting the wavenumber of the fibrous material. The solutions for the acoustic pressure and the particle velocity in x direction may be expressed as

$$P_B(r,x) = \sum_{n=0}^{\infty} (B_n^+ e^{-jk_{x,B,n}x} + B_n^- e^{jk_{x,B,n}x})\psi_{B,n,P}(r) \tag{11}$$

and

$$u_{x,B}(r,x) = \frac{1}{\rho_0\omega}\sum_{n=0}^{\infty} k_{x,B,n}(B_n^+ e^{-jk_{x,B,n}x} - B_n^- e^{jk_{x,B,n}x})\psi_{B,n,u_x}(r) \tag{12}$$

with $k_{x,B,n}$ being the common wavenumber in the axial direction for both the air and fiber, which satisfies the characteristic equation

$$\frac{\rho_0 \tilde{k}_{r,B,n}}{\tilde{\rho} k_{r,B,n}} \frac{\mathrm{J}_0(k_{r,B,n} r_2)}{\mathrm{J}_1(k_{r,B,n} r_2)} = \frac{\mathrm{J}_0(\tilde{k}_{r,B,n} r_2) Y_1(\tilde{k}_{r,B,n} r_3) - Y_0(\tilde{k}_{r,B,n} r_2) \mathrm{J}_1(\tilde{k}_{r,B,n} r_3)}{\mathrm{J}_1(\tilde{k}_{r,B,n} r_2) Y_1(\tilde{k}_{r,B,n} r_3) - Y_1(\tilde{k}_{r,B,n} r_2) \mathrm{J}_1(\tilde{k}_{r,B,n} r_3)} \tag{13}$$

with Y_0, Y_1, and J_1 being the zeroth order Neumann, first order Neumann, and first order Bessel functions, respectively;

$$k_{r,B,n} = \sqrt{k_0^2 - k_{x,B,n}^2} \tag{14a}$$

and

$$\tilde{k}_{r,B,n} = \sqrt{\tilde{k}^2 - k_{x,B,n}^2} \tag{14b}$$

the wavenumbers in the radial direction for the air and fiber, respectively; and

$$\psi_{B,n,P}(r) = \begin{cases} \mathrm{J}_0(k_{r,B,n} r), & 0 \leqslant r \leqslant r_2, \\ D\left[\mathrm{J}_0(\tilde{k}_{r,B,n} r) - \dfrac{\mathrm{J}_1(\tilde{k}_{r,B,n} r_3)}{Y_1(\tilde{k}_{r,B,n} r_3)} Y_0(\tilde{k}_{r,B,n} r)\right], & r_2 \leqslant r \leqslant r_3, \end{cases} \tag{15a}$$

$$\psi_{B,n,u_x}(r) = \begin{cases} \mathrm{J}_0(k_{r,B,n} r), & 0 \leqslant r \leqslant r_2, \\ \dfrac{\rho_0}{\tilde{\rho}} D\left[\mathrm{J}_0(\tilde{k}_{r,B,n} r) - \dfrac{\mathrm{J}_1(\tilde{k}_{r,B,n} r_3)}{Y_1(\tilde{k}_{r,B,n} r_3)} Y_0(\tilde{k}_{r,B,n} r)\right], & r_2 \leqslant r \leqslant r_3 \end{cases} \tag{15b}$$

are the eigenfunctions with

$$D = \frac{\mathrm{J}_0(k_{r,B,n} r_2) Y_1(\tilde{k}_{r,B,n} r_3)}{\mathrm{J}_0(\tilde{k}_{r,B,n} r_2) Y_1(\tilde{k}_{r,B,n} r_3) - \mathrm{J}_1(\tilde{k}_{r,B,n} r_3) Y_0(\tilde{k}_{r,B,n} r_2)}.$$

With the expressions of pressure and velocity of inlet, outlet, and expansion chamber [Eqs. (2), (6)–(8), (11), and (12)], the unknown coefficients A_n, B_n, and C_n are then determined by using the boundary conditions at the expansion ($x = 0$) and contraction ($x = L$). The continuities of the acoustic pressure and the velocity across the interface reveal that

$$P_A = P_B \quad \text{for } 0 \leqslant r \leqslant r_1, x = 0, \tag{16}$$

$$u_B = \begin{cases} u_A & \text{for } 0 \leqslant r \leqslant r_1, x = 0, \\ 0 & \text{for } r_1 \leqslant r \leqslant r_3, x = 0, \end{cases} \tag{17}$$

$$P_C = P_B \quad \text{for } 0 \leqslant r \leqslant r_1, x = L, \tag{18}$$

$$u_B = \begin{cases} u_C & \text{for } 0 \leqslant r \leqslant r_1, x = L, \\ 0 & \text{for } r_1 \leqslant r \leqslant r_3, x = L, \end{cases} \tag{19}$$

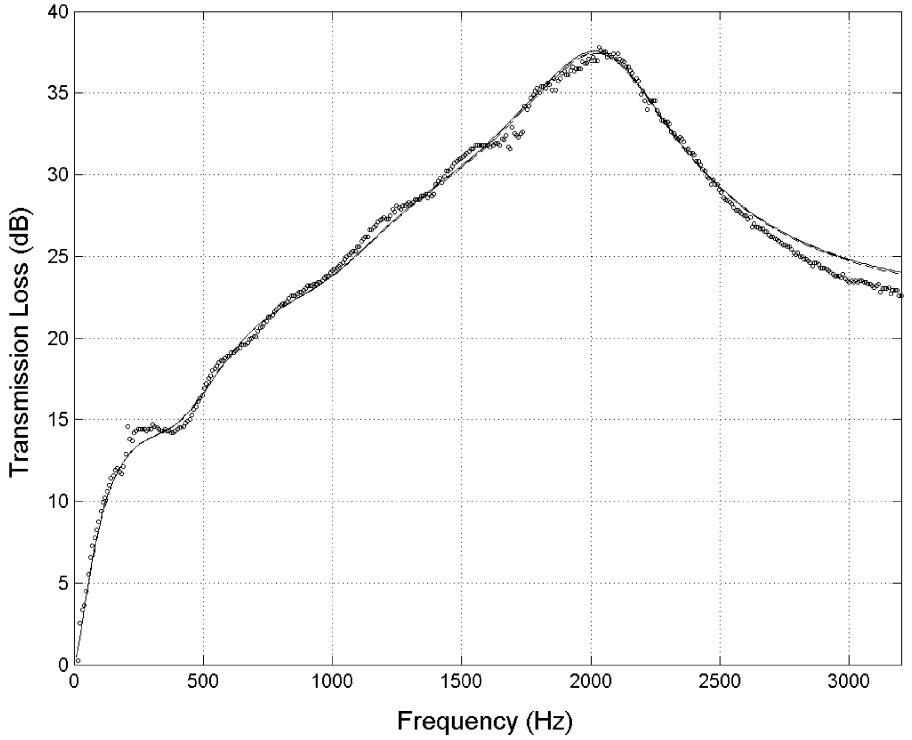

Fig. 2. Transmission loss of dissipative expansion chamber with $r_2 = 3.50$ cm, $r_3 = 8.22$ cm, and $R = 4896$ Rayls/m: ——, analytical with $N = 8$; - - - - , analytical with $N = 10$; –·–·–·–, BEM; ◦, experimental.

or, in view of Eqs. (2), (6)–(8), and (11)–(12),

$$\sum_{n=0}^{\infty} (A_n^+ + A_n^-)\psi_{A,n}(r) = \sum_{n=0}^{\infty} (B_n^+ + B_n^-)\psi_{B,n,P}(r) \quad \text{for } 0 \leqslant r \leqslant r_1, \tag{20}$$

$$\sum_{n=0}^{\infty} k_{x,B,n}(B_n^+ - B_n^-)\psi_{B,n,u_x}(r) = \begin{cases} \sum_{n=0}^{\infty} k_{x,A,n}(A_n^+ - A_n^-)\psi_{A,n}(r) & \text{for } 0 \leqslant r \leqslant r_1, \\ 0 & \text{for } r_1 \leqslant r \leqslant r_3, \end{cases} \tag{21}$$

$$\sum_{n=0}^{\infty} (C_n^+ + C_n^-)\psi_{C,n}(r) = \sum_{n=0}^{\infty} (B_n^+ \mathrm{e}^{-\mathrm{j}k_{x,B,n}L} + B_n^- \mathrm{e}^{\mathrm{j}k_{x,B,n}L})\psi_{B,n,P}(r) \quad \text{for } 0 \leqslant r \leqslant r_1, \tag{22}$$

$$\sum_{n=0}^{\infty} k_{x,B,n}(B_n^+ \mathrm{e}^{-\mathrm{j}k_{x,B,n}L} + B_n^- \mathrm{e}^{\mathrm{j}k_{x,B,n}L})\psi_{B,n,u_x}(r) = \begin{cases} \sum_{n=0}^{\infty} k_{x,C,n}(C_n^+ - C_n^-)\psi_{C,n}(r) & \text{for } 0 \leqslant r \leqslant r_1, \\ 0 & \text{for } r_1 \leqslant r \leqslant r_3. \end{cases} \tag{23}$$

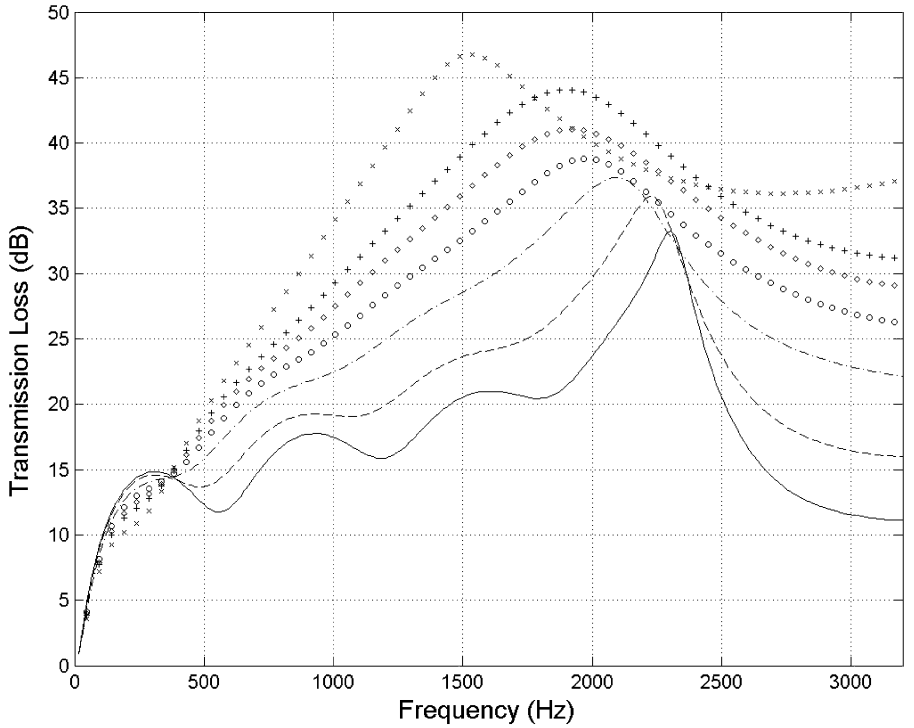

Fig. 3. Transmission loss for different fiber resistivity with $r_2 = 3.50$ cm, and $r_3 = 8.22$ cm: ——, $R = 1000$ Rayls/m; - - - -, $R = 2000$ Rayls/m; –·–·–·–, $R = 4000$ Rayls/m; ◦, $R = 6000$ Rayls/m; ◇, $R = 8000$ Rayls/m; +, $R = 10,000$ Rayls/m; ×, $R = 20,000$ Rayls/m.

By imposing the continuities of the axial velocity/pressure integral over discrete zones at the interfaces, Eqs. (20)–(23) yield

$$\sum_{n=0}^{N} (A_n^+ + A_n^-) \int_0^{r_{m,P}} \psi_{A,n}(r)\,\mathrm{d}r = \sum_{n=0}^{N} (B_n^+ + B_n^-) \int_0^{r_{m,P}} \psi_{B,n,P}(r)\,\mathrm{d}r, \tag{24}$$

$$\sum_{n=0}^{N} k_{x,B,n}(B_n^+ - B_n^-) \int_0^{r_{m,u}} \psi_{B,n,u_x}(r)\,\mathrm{d}r = \begin{cases} \sum_{n=0}^{N} k_{x,A,n}(A_n^+ - A_n^-) \int_0^{r_{m,u}} \psi_{A,n}(r)\,\mathrm{d}r & \text{for } 0 \leqslant r_{m,u} \leqslant r_1, \\ \sum_{n=0}^{N} k_{x,A,n}(A_n^+ - A_n^-) \int_0^{r_1} \psi_{A,n}(r)\,\mathrm{d}r & \text{for } r_1 \leqslant r_{m,u} \leqslant r_3, \end{cases} \tag{25}$$

$$\sum_{n=0}^{N} (C_n^+ + C_n^-) \int_0^{r_{m,P}} \psi_{C,n}(r)\,\mathrm{d}r = \sum_{n=0}^{N} (B_n^+ \mathrm{e}^{-\mathrm{j}k_{x,B,n}L} + B_n^- \mathrm{e}^{\mathrm{j}k_{x,B,n}L}) \int_0^{r_{m,P}} \psi_{B,n,P}(r)\,\mathrm{d}r, \tag{26}$$

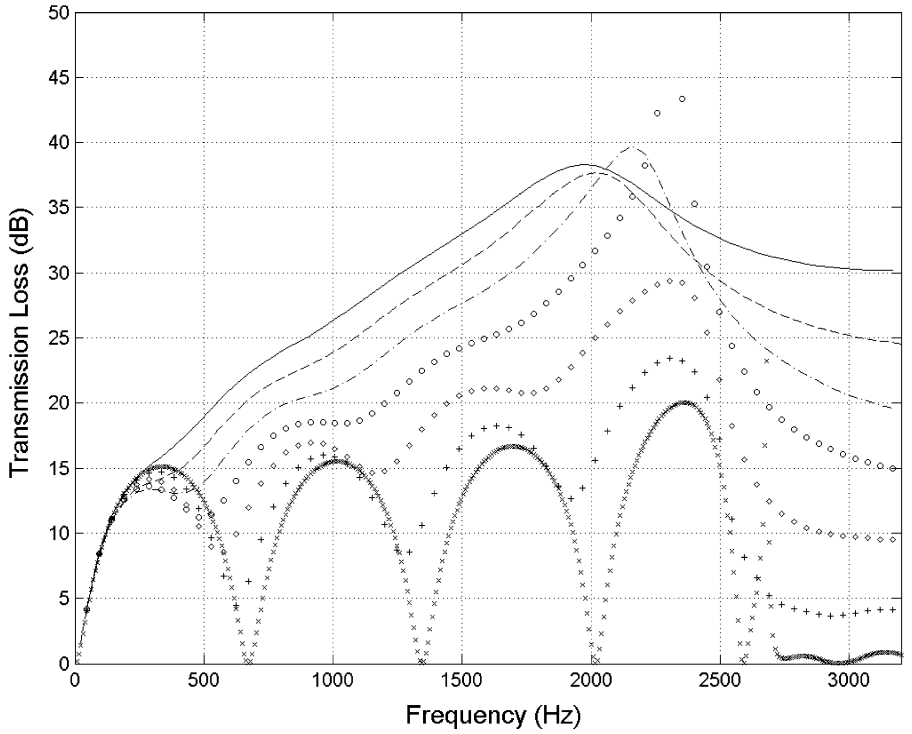

Fig. 4. Transmission loss for different fiber thickness with $r_3 = 8.22$ cm, and $R = 4896$ Rayls/m: ——, $r_2 = r_1$; - - - -, $r_2 = 3.5$ cm; –·–·–·–, $r_2 = 4.5$ cm; ◦, $r_2 = 5.5$ cm; ◇, $r_2 = 6.5$ cm; +, $r_2 = 7.5$ cm; ×, $r_2 = r_3$ (no fiber).

$$\sum_{n=0}^{N} k_{x,B,n}(B_n^+ \mathrm{e}^{-\mathrm{j}k_{x,B,n}L} - B_n^- \mathrm{e}^{\mathrm{j}k_{x,B,n}L}) \int_0^{r_{m,u}} \psi_{B,n,u_x}(r)\,\mathrm{d}r$$

$$= \begin{cases} \sum_{n=0}^{N} k_{x,C,n}(C_n^+ - C_n^-) \int_0^{r_{m,u}} \psi_{C,n}(r)\,\mathrm{d}r & \text{for } 0 \leqslant r_{m,u} \leqslant r_1, \\ \sum_{n=0}^{N} k_{x,C,n}(C_n^+ - C_n^-) \int_0^{r_1} \psi_{C,n}(r)\,\mathrm{d}r & \text{for } r_1 \leqslant r_{m,u} \leqslant r_3 \end{cases} \tag{27}$$

with

$$r_{m,P} = \frac{m}{N+1} r_1, \quad m = 1, \ldots, N+1, \tag{28}$$

$$r_{m,u} = \frac{m}{N+1} r_3, \quad m = 1, \ldots, N+1. \tag{29}$$

To determine the transmission loss of the dissipative expansion silencer, it is assumed that: (1) the incoming wave is planar and A_0^+ is set to be unity; and (2) an anechoic termination is imposed at the exit by setting C_n^- to zero. With the $4(N+1)$ coefficients solved in Eqs. (24)–(27), the transmission loss is then determined as

$$TL = -20 \log_{10} |C_0^+|. \tag{30}$$

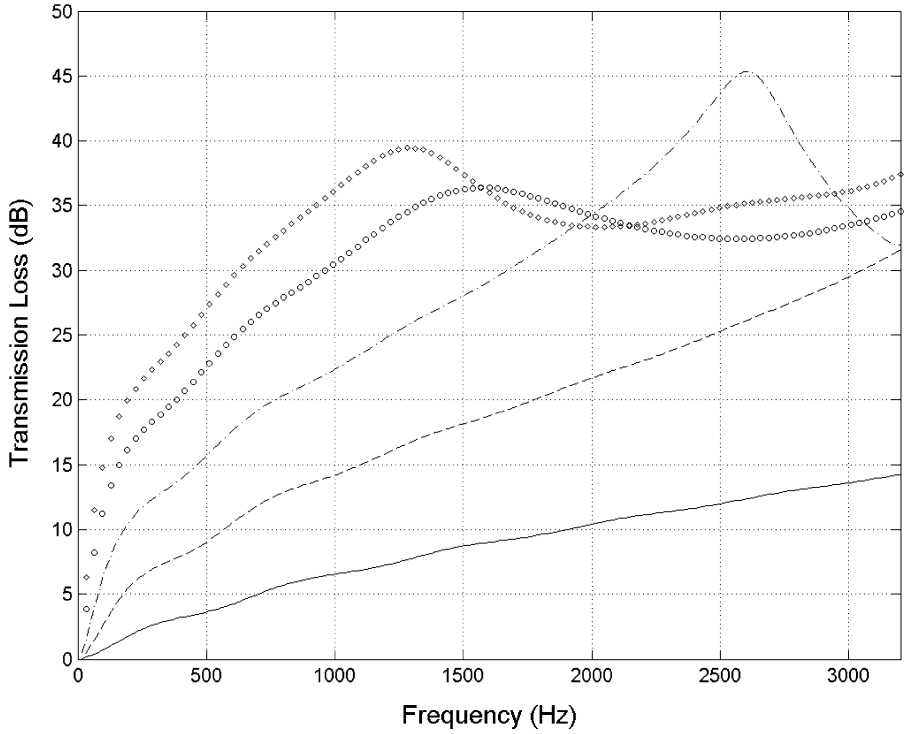

Fig. 5. Transmission loss for different area ratio m with $r_2 = r_1$ and $R = 4896$ Rayls/m: ——, $m = 2$; - - - -, $m = 4$; –·–·–·–, $m = 8$; ◦, $m = 16$; ◇, $m = 25$.

3. Results

A dissipative expansion silencer has been fabricated with $r_1 = 2.45$ cm, and $L = 25.72$ cm. The characteristic impedance $\tilde{Z} = \tilde{\rho}\tilde{c}$ and the wavenumber $\tilde{k}$ of the absorbing material in the present study is given as [10]

$$\frac{\tilde{Z}}{Z_0} = [1 + 0.0855(f/R)^{-0.754}] + \mathrm{j}[-0.0765(f/R)^{-0.732}], \tag{31}$$

$$\frac{\tilde{k}}{k} = [1 + 0.1472(f/R)^{-0.577}] + \mathrm{j}[-0.1734(f/R)^{-0.595}] \tag{32}$$

with $Z_0 = \rho_0 c_0$ being the characteristic impedance of the air, and f(Hz) denotes frequency and R(mks Rayls/m) the resistivity of the absorbing material.

The transmission loss results from the analytical approach with different number of higher order modes are compared with BEM predictions and measurements in Fig. 2 with $r_2 =$ 3.50 cm, $r_3 = 8.22$ cm, and $R = 4896$ Rayls/m, which corresponds to a filling density of 100 g/l. The details of the BEM and experimental approaches are elaborated in Refs. [8,11]. With $N \geqslant 8$, all three sets are in good agreement.

Fig. 3 depicts the analytical transmission loss results for different fiber flow resistivity for $r_2 = 3.50$ cm and $r_3 = 8.22$ cm. Higher fiber resistivity leads to higher transmission loss at medium

to high frequencies, while the lower resistivity improves transmission loss at low frequencies. The fiber flow resistivity may therefore depend on the application.

With $R = 4896$ Rayls/m and $r_3 = 8.22$ cm, Fig. 4 examines the effect of variation of fiber thickness, $r_3 - r_2$, on the transmission loss. The results for the empty silencer are also included. The overall performance of the silencer is generally improved by increasing fiber thickness. Thus, for maximum attenuation, the diameters for the airway and inlet/outlet pipes in the dissipative silencer would be the same.

With $r_2 = r_1$ and $R = 4896$ Rayls/m, Fig. 5 investigates the effect of variation of area ratio $m = (r_3/r_1)^2$ on the transmission loss. Higher area ratio improves the performance of dissipative expansion silencer at low to medium frequencies. Such a trend may be reversed locally at higher frequencies and higher area ratios. Currently, an effort is under way to develop an analytical solution for dissipative chambers with empty space between fiber filling and outer housing.

References

[1] P.M. Morse, Transmission of sound inside pipes, *Journal of the Acoustical Society of America* 11 (1939) 205–210.
[2] R.A. Scott, The propagation of sound between walls of porous material, *Proceedings of the Physical Society* 58 (1946) 358–368.
[3] S.H. Ko, Theoretical analyses of sound attenuation in acoustically lined flow ducts separated by porous splitters (rectangular, annular and circular ducts), *Journal of Sound and Vibration* 39 (1975) 471–487.
[4] A. Cummings, I.J. Chang, Internal mean flow effects on the characteristics of bulk-reacting liners in circular ducts, *Acustica* 64 (1987) 169–178.
[5] A. Cummings, I.J. Chang, Sound attenuation of a finite length dissipative flow duct silencer with internal mean flow in the absorbent, *Journal of Sound and Vibration* 127 (1988) 1–17.
[6] K.S. Peat, A transfer-matrix for an absorption silencer element, *Journal of Sound and Vibration* 146 (1991) 353–360.
[7] A. Selamet, I.J. Lee, Z.L. Ji, N.T. Huff, Acoustic attenuation performance of perforated concentric absorbing silencers, *SAE Noise and Vibration Conference and Exposition*, SAE Paper No. 2001-01-1435, Traverse City, MI, April 30–May 3, 2001.
[8] A. Selamet, I.J. Lee, N.T. Huff, Acoustic attenuation of hybrid silencers, *Journal of Sound and Vibration* 262 (2003) 509–527.
[9] M.L. Munjal, Analysis and design of pod silencers, *Journal of Sound and Vibration* 262 (2003) 497–507.
[10] M. Nice, Owens Corning Automotive, Internal Report, 1999.
[11] A. Selamet, N.S. Dickey, J.M. Novak, Herschel–Quincke tube: a theoretical, computational, and experimental investigation, *Journal of the Acoustical Society of America* 96 (1994) 3177–3185.